Journal of Solid State Chemistry **164,** 354–360 (2002)
doi:10.1006/jssc.2001.9505, available online at http://www.idealibrary.com on IDEAL®

Hydrothermal Synthesis, Structure, and Magnetic Properties of a Layered Fe(III) Carboxymethylphosphonate: $[Fe(H_2O)(O_3P–CH_2–CO_2)]$ or MIL-49

Morgane Sanselme, Myriam Riou-Cavellec,[1] Jean-Marc Grenèche,* and Gérard Férey

*Institut Lavoisier, UMR CNRS 8637, Université de Versailles-St Quentin en Yvelines, 45 avenue des Etats-Unis, 78035 Versailles Cedex, France; and *Laboratoire de Physique de l'Etat Condensé, UMR CNRS 6087, Université du Maine, Avenue O. Messiaen, 72085 Le Mans Cedex 9, France*

Received September 28, 2001; in revised form December 26, 2001; accepted January 4, 2002

$[Fe^{III}(H_2O)(O_3P–(CH_2)–CO_2)]$ or MIL-49 was hydrothermally synthesized under autogenous pressure at 170°C for 48 h. Its bidimensional structure was solved from single-crystal X-ray diffraction in the monoclinic space group $P2_1/c$ (No.14). Cell parameters are a = 9.3836(3) Å, b = 6.3798(3) Å, c = 10.1371(3) Å, β = 111.891(2)°, Z = 4, and V = 563.10(4) Å^3. Reliability factors of the structure refinement are $R_1(F)$ = 0.0470 and $wR_2(F^2)$ = 0.1297 for 1036 reflections with $I > 2\sigma(I)$. The structure of MIL-49 is based on inorganic units built up from two edge-sharing $[FeO_5(H_2O)]$ octahedra and two carboxymethylphosphonate groups. The connection of these units leads to the formation of hybrid sheets. A dangling oxygen atom from the carboxy function points toward the interlayer space and is responsible for hydrogen bonding with adjacent layers. Magnetic measurements and ^{57}Fe Mössbauer study reveal an antiferromagnetic ordering below T_N = 25(1) K which becomes canted below 11(1) K.

Key Words: **hydrothermal synthesis; iron carboxymethylphosphonate; structure; magnetism.**

INTRODUCTION

Many organically templated metallophosphates (*Me* = Al, Ga, Fe, etc.) with open frameworks have been synthesized since the discovery of AlPO's in 1982 (1, 2). In these phases, the microporous structure appears after extraction of the organic template, but in many cases thermal treatment of these compounds induces collapse of the inorganic skeleton. Thus, the synthesis of hybrid open framework materials free of templated molecules is promising and overcomes this difficulty (3–5).

Recently, we obtained by hydrothermal synthesis new hybrid organic–inorganic compounds using *n*-carboxylates (6) or diphosphonates (7) as complexing agents of several metallic cations (Ln, Co, Fe, V, Ni, Ti, etc.). Up to now, the use of bifunctional carboxyethylphosphonic acid led to the synthesis of many 2D (8) or 3D (9) hybrid materials also based on various cations (Fe, V, Sn, Co, Pr, etc.). However, a few carboxymethylphosphonates have been described in the literature (10); they can also adopt two- or three-dimensional structures including cations such as Mn, Al, and Zn. In this article, we present the layered structure and the magnetic properties of the first iron carboxymethylphosphonate labeled MIL-49.

[1]To whom correspondance should be addressed. E-mail: cavellec@chimie.uvsq.fr. Fax: (33) (0) 1 39 25 43 58.

EXPERIMENTAL

Synthesis

$[Fe^{III}(H_2O)(O_3P–(CH_2)–CO_2)]$ or MIL-49 was synthesized hydrothermally from iron fine powder (Riedel-de-Haën, 99 + %), carboxymethylphosphonic acid (Epsilon chimie), and demineralized water. The molar ratios in the initial mixture were 1 Fe^0 (0.0311 g):2 $H_2O_3P–(CH_2)–CO_2H$ (0.1556 g):500 H_2O (5 mL). The initial pH of the mixture was ca. 1. Reactants were introduced into a Teflon lined vessel, then sealed in a Parr acid digestion bomb. The latter was heated at 170°C for 48 h under autogenous pressure. At the end of the reaction, the pH of the solution remains acidic; the resulting product was filtered off, washed with water, and dried at room temperature. It was quite homogenous and consisted of some aggregates of thin white needles (Fig. 1).

Physical Methods

Semiquantitative EDX analysis of some crystals (performed on a JEOL 5800 LV scanning microscope equipped with Oxford Linkisis analyzer) gave a Fe/P ratio equal to ca. 1. Elemental analysis results indicated (wt%):Fe, 25.65

0022-4596/02 $35.00

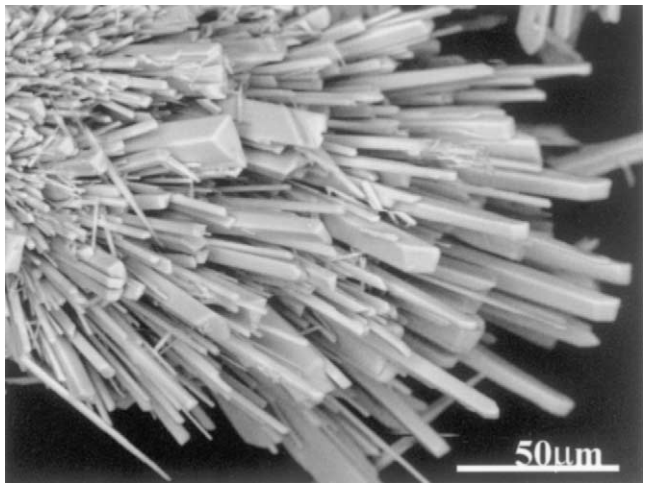

FIG. 1. Scanning electronic micrograph of crystals of MIL-49.

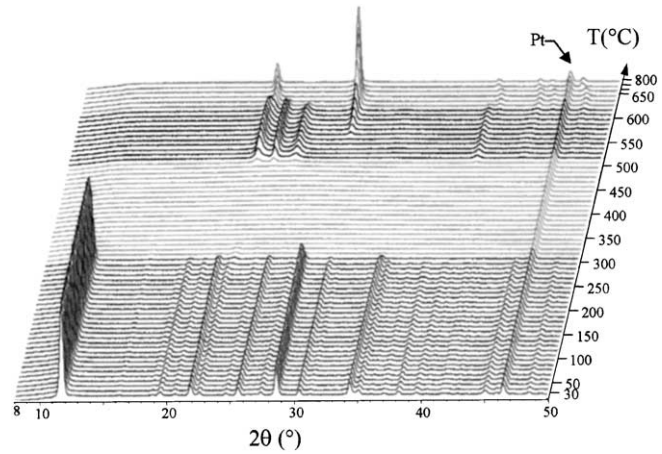

FIG. 3. Thermodiffractogram of MIL-49 showing the stability of the structure up to 300°C.

(calcd:26.56); P, 14.48 (calcd:14.69); C, 11.58 (calcd:11.37), thus confirming the atomic ratio 1Fe:1P:1C.

The experimental density d_{exp} = 2.51(1) (Micromeritics 1330 Accupyc pycnometer) is close to the theoretical one d_{calc} = 2.49.

TGA measurements of the title compound were performed under O_2 gas flow (using a TA Instrument Type 2050 analyzer) at 5°C min^{-1} from 25 to 900°C. We observe a quasi-continuous weight loss beginning at ca. 300°C (Fig. 2). It includes the departure of a coordinated water molecule and the calcination of the organic species. At 900°C, residual $FePO_4$ recrystallizes (11). The experimental weight loss (28.95%) is in agreement with the theoretical one (28.44%). TGA analysis of MIL-49 was confirmed by thermodiffractometry, performed on a D5000 Siemens powder thermodiffractometer ($\lambda_{CoK\alpha}$) (equipped with an Anton Parr Furnace) at the following heating rates: 5°C/min with a 10°C step in the range 30–650°C and 50°C step in the range 650–800°C. According to Fig. 3, MIL-49 is stable up to 300°C; at 500°C, an intermediate phase appears, but it remains unidentified. Finally, $FePO_4$ is obtained from 650°C.

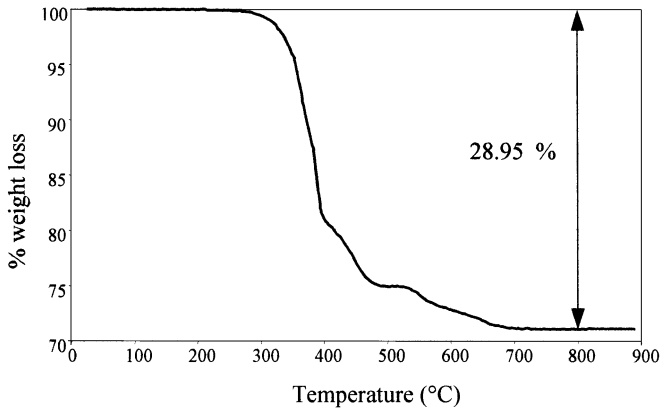

FIG. 2. TGA curve under O_2 gas flow.

Structure Determination

A suitable single crystal ($0.540 \times 0.04 \times 0.020\,mm^3$) was used for X-ray data collection on a Siemens-type SMART three-circle diffractometer equipped with a CCD detector (exposure time: 30 s per frame). An absorption correction specifically for the CCD detector was applied to all data using the SADABS program (12).

The structure of MIL-49 was solved in the centrosymmetric space group $P2_1/c$ (No. 14) by direct methods using the TREF option of the SHELXTL crystallographic software package (13). The heaviest atoms (Fe, P) were located first; the remaining atoms (O, C) were deduced from Fourier-difference map calculations. Hydrogen atoms H(1a) and H(1b) from the CH_2 group (i.e., bonded to C(1) atom) were localized applying geometrical constraints (HFIX 23). At the end of the refinement cycle, the two highest residual peaks (1 and 0.8 e Å^{-3}) were less than 1 Å from O(3)^w: these atoms were introduced as hydrogen atoms H(2)^w and H(3)^w from the terminal water molecule (H(2)^w–O(3)^w–H(3)^w = 101°). All atoms except hydrogen atoms were refined with anisotropic thermal factors. Refinements with 1471 unique reflections (R_{int} = 0.0462) led to $R_1(F)$ = 0.0470 and wR_2 (F^2) = 0.1113 for 1036 reflections with $I > 2\sigma(I)$.

Conditions of data collection, atomic coordinates, and principal bond lengths and angles are given in Tables 1, 2, and 3 respectively.

TABLE 1
Crystal Data and Structure Refinement for MIL-49

Formula	$[Fe(H_2O)(O_3P–CH_2–COO)]$
Formula weight	$211\,g\,mol^{-1}$
Wavelength (Mo$K\alpha$)	0.71073 Å
Crystal system	Monoclinic
Space group	$P2_1/c$ (No. 14)
a	9.3836(3) Å
b	6.3798(3) Å
c	10.1371(4) Å
β	111.891(2) Å
Volume	563.10(4) $Å^3$
Z	4
Density	
Calculated	2.49
Measured	2.51(1)
Temperature	25°C
Absorption coefficient	$2.927\,mm^{-1}$
$F(000)$	420
Crystal size (mm^3)	0.540 × 0.04 × 0.020
θ range for data collection	$2.34 \le \theta \le 29.73$
Limiting indices	$-12 \le h \le 8$; $-8 \le k \le 8$; $-13 \le l \le 14$
Reflections collected	3789 (30 s/frame)
Independent reflections	1471 [R(int) = 0.0462]
Refinement methods	Full-matrix least-squares on F^2
Data/restraints/parameters	1471/0/99
Goodness of fit on F^2	0.952
Final R indices [$I>2\sigma$ (I)]	R_1 = 0.0470, wR_2 = 0.1113
R indices [all data]	R_1 = 0.0784; wR_2 = 0.1297
Largest diff. peak and hole	0.750 and $-1.435\ e\ Å^{-3}$

Magnetic Measurements and ^{57}Fe Mössbauer Spectrometry

The magnetization (M) of MIL-49 was measured as a function of the applied field at many temperatures in the range 2 to 300 K with a Quantum Design Squid device.

Mössbauer experiments were carried out at 300, 77, and 4.2 K by means of a bath cryostat, using a constant acceleration spectrometer and a Co source diffused in a Rh matrix. The values of the isomer shifts are quoted relative to α-Fe foil at 300 K. The hyperfine parameters were refined using a least-squares fitting procedure in the MOSFIT program (14).

RESULTS AND DISCUSSION

Structural Description

$[Fe^{III}(H_2O)(O_3P–CH_2–COO)]$ or MIL-49 can be described as the stacking of inorganic organic sheets along [100] (Fig. 4). These layers are built up from units based on two edge-sharing $[FeO_5(H_2O)]$ octahedra and two carboxymethylphosphonate moieties (Fig. 5). In each dimer, the octahedra share the O(1)–O(1) edge and present a terminal water molecule ($H(2)^w$–$O(3)^w$–$H(3)^w$). The $[PO_3C]$ tetrahedral extremities from carboxymethylphosphonate groups are connected on the octahedral dimers via O(1) apices, whereas the carboxylate ligands are bonded to the Fe(III) octahedra via O(4) atoms. The carboxylate function also displays a non-bonded O(6) atom.

TABLE 2
Atomic Coordinates and Equivalent Isotropic Displacement Parameters (Å)[a]

	x	y	z	u_{eq}
Fe	0.8981(1)	0.1637(1)	0.5512(1)	0.012(1)
P	0.1328(1)	0.3296(2)	0.3963(1)	0.012(1)
O(1)	0.0596(4)	0.1585(5)	0.4614(3)	0.012(1)
O(2)	0.0556(4)	0.1712(6)	0.7370(3)	0.021(1)
$O(3)^w$	0.7309(4)	0.1376(5)	0.3493(4)	0.018(1)
O(4)	0.7391(4)	0.1024(5)	0.6301(4)	0.020(1)
O(5)	0.1336(4)	0.5401(5)	0.4655(4)	0.019(1)
O(6)	0.5628(5)	−0.0427(6)	0.6949(4)	0.028(1)
C(1)	0.3293(6)	0.2562(8)	0.4388(5)	0.018(1)
C(2)	0.6539(6)	−0.0556(8)	0.6338(6)	0.018(1)
H(1a)	0.3818(6)	0.3685(8)	0.4109(5)	0.021(1)
H(1b)	0.3786(6)	0.2385(8)	0.5409(5)	0.021(1)
$H(2)^w$	0.6317(6)	0.147(8)	0.3412(5)	0.022(1)
$H(3)^w$	0.732(6)	0.204(9)	0.2849(6)	0.032(1)

[a] U(eq) is defined as one-third of the trace of the orthogonalized U_{ij} tensor. Supercript "w" indicates the terminal water molecule

The so-built units are then connected in such a way that each $[PO_3C]$ tetrahedron shares three oxygen vertices with three different dimers within a layer. The dangling O(6) atoms are then responsible for the cohesion of the structure by developing hydrogen bonds with the terminal water molecules of $[FeO_5(H_2O)]$ octahedra from a neighboring layer: $O(6)\cdots H(2)^w–O(3)^w = 2.87$ Å; $O(6)\ –H(2)^w–O(3)^w = 153.8°$. Bond valence calculations (15) indicate 3.1 valence units from Fe(III) in agreement with the observed Fe^{III}–O bond lengths ranging from 1.913 to 2.109 Å.

IR spectroscopic study (Nicolet Magna IR 550) of MIL-49 displays two bands (broad at 3188 cm^{-1} and sharp at

TABLE 3
Principal Bond Lenghts (Å) and Angles (°) in MIL-49

$[Fe(H_2O)O_5]$ octahedron			
Fe–O(5)	1.913 (3)		
Fe–O(2)	1.915 (3)		
Fe–O(4)	1.977 (3)		
Fe–O(1)	2.039 (3)		
$Fe–O(3)^w$	2.061 (3)		
Fe–O(1)	2.109 (3)		
Within $[O_3P–C(1)H_2–C(2)O_2]^{3-}$ organic moiety			
P–O(2)	1.502 (3)	O(6)–C(2)–O(4)	120.8 (5)
P–O(5)	1.512 (3)	O(6)–C(2)–C(1)	121.5 (4)
P–O(1)	1.558 (3)	O(4)–C(2)–C(1)	117.7 (4)
P–C(1)	1.795 (5)		
C(1)–C(2)	1.511 (6)		
C(2)–O(4)	1.298 (5)		
C(2)–O(6)	1.228 (5)		

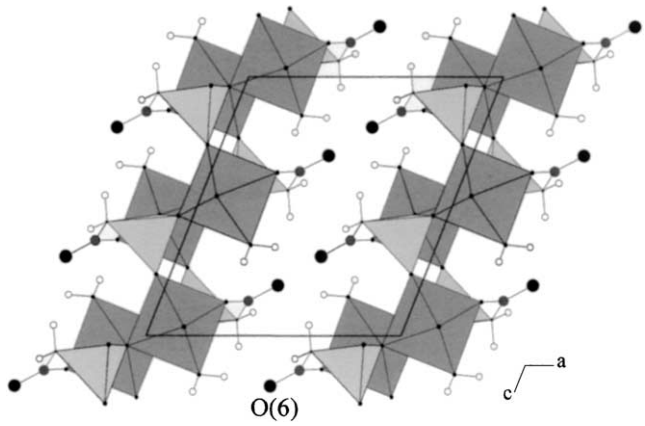

FIG. 4. Projection of the structure along [010] displaying the layered character of MIL-49. The strongest hydrogen bonds are represented as dashed lines between dangling O(6) atoms from carboxylate groups and H atoms from coordinated water molecules.

1689 cm^{-1}) which are due respectively to the $\nu_{(O-H)}$ and the $\delta_{(H-O-H)}$ deformation bands of water molecules. A sharp band at 1632 cm^{-1}, close to the value proposed by Nakamoto (16), corresponds to $\nu_{C=O\ldots HO}$ and confirms the deprotonation of the carboxylate group.

In the literature, structures of Al^{3+} (10a), Zn^{2+} (10b), and Mn^{2+} (10c) carboxymethylphosphonates differ from that of MIL-49 (Fe^{3+}). However, except for the zeolite-like 3D zinc compound synthesised by Stucky *et al.*, common features are observed. In the 2D $[Al(O_3PCH_2COO)\cdot 3H_2O]$ compound (10a), both oxygen atoms from the carboxylate function present analogies with those of MIL-49: one oxygen is ligand to the metallic (+III) cation whereas the other remains dangling in the interlayer space. In the 3D $[Mn_3(O_3PCH_2COO)_2]$ compound (10c), on three different crystallographic Mn^{2+} sites, one forms with the organic moieties the same subunits that the one encountered in MIL-49 does. However, although the second oxygen from carboxylate function is deprotonated, it is ligand of the two other Mn^{2+} cations and this leads to the 3D structure.

Among synthesized iron-based hybrid materials, we have already observed this 3D character induced by the connection of both carboxylate oxygen atoms to metallic Fe^{2+} cations (MIL-38 (9f) or MIL-45 (6d)); but when iron is only at the oxidation state (+III) in the compound (MIL-37(8g), MIL-49), we get, up to now, exclusively 2D materials with dangling carboxylate oxygen atoms in the interlayer space.

Magnetism Results and ^{57}Fe Mössbauer Study

The Mössbauer spectra of MIL-49 recorded at 300 and 77 K exhibit a quadrupolar hyperfine structure with narrow lines (Fig. 6). They can be well described using a single quadrupolar component that is in agreement with the

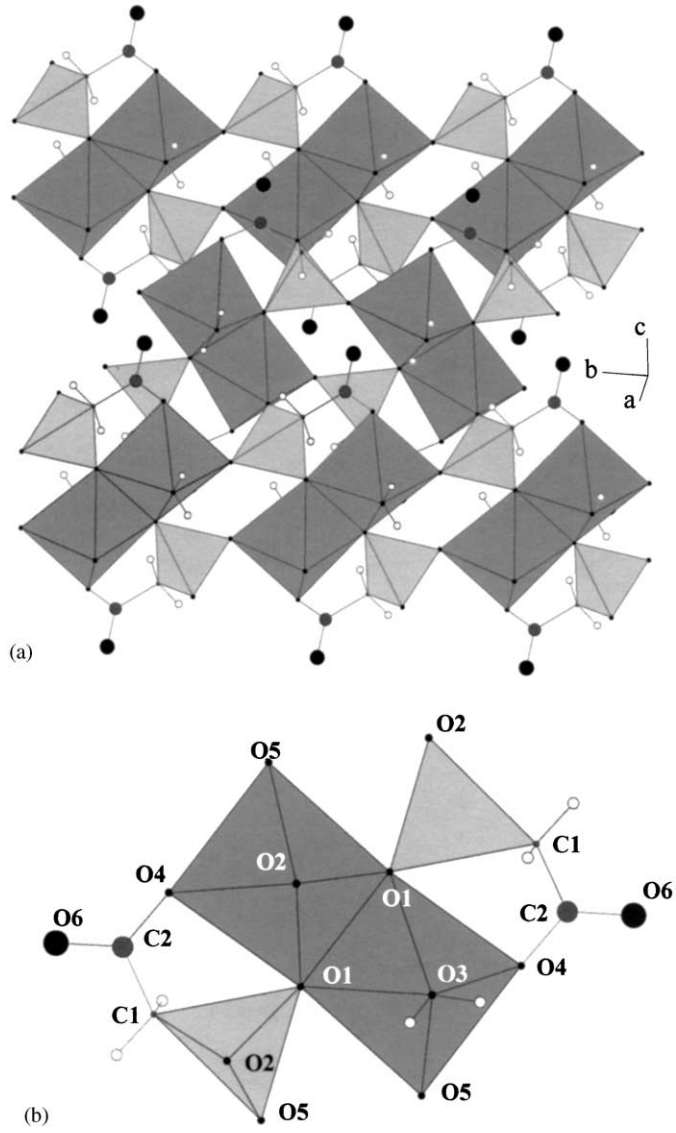

FIG. 5. (a) Hybrid layer of MIL-49. (b) Building unit of the layer.

existence of a single Fe site as observed from the crystallographic structure determined at 298 K. The weak asymmetrical shape of the doublet is due to a texture effect which has been checked after rotating the sample with respect to the γ-beam direction. Indeed such a small preferential orientation of the powdered sample originates from its layered structure. The refined values of hyperfine parameters which are listed in Table 4 are consistent with a single Fe^{3+} site in high-spin state.

At 4.2 K, the spectrum (Fig. 6) exhibits unambiguously a magnetic hyperfine structure resulting from two sextets that is consistent neither with the results observed in the paramagnetic range, nor with the crystallographic structure at 298 K. It is important to note that the paramagnetic spectra can be also described by two equiprobable

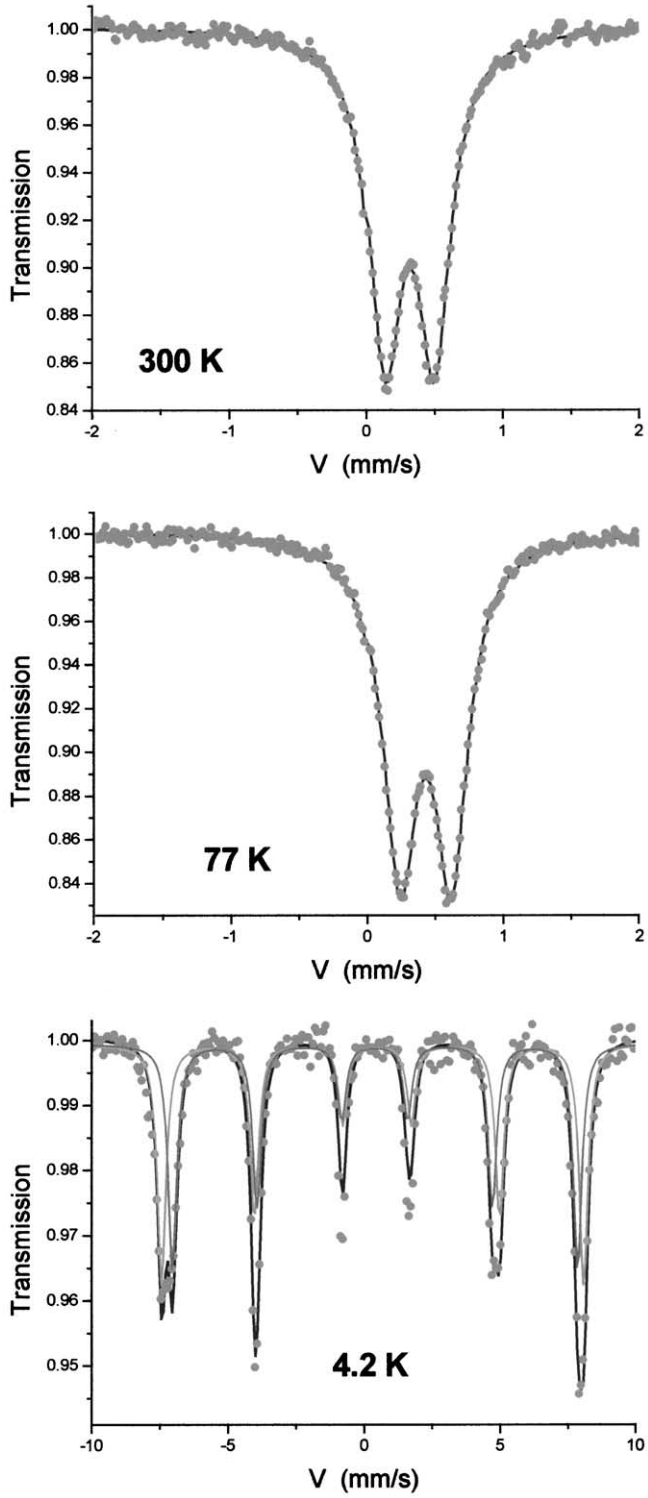

FIG. 6. Mössbauer spectra at 300, 77, and 4.2 K.

quadrupolar components, but the hyperfine parameters remain very similar in agreement with the presence of a single iron site, as previously discussed. The refined values of hyperfine parameters at low temperature are listed in Table 4. They reveal that the hyperfine field values (i) weakly differ one from another and (ii) are rather low, compared with values expected for iron-containing oxides, but they are in good agreement with other solids with clusters of Fe(III). The presence of two magnetic iron sites with a 1:1 ratio indicates a magnetostriction related to a possible lowering of symmetry close to T_N. The existence of two iron sites might originate from a passage to a noncentric monoclinic space group or to the centric triclinic space group.

TABLE 4
Hyperfine Parameters at 300, 77, and 4.2 K[a]

Temperature (K)	IS (mm/s) ±0.02	Γ (mm/s) ±0.02	SQ or 2ε (mm/s) ±0.02	H_{hyp} (T) ±0.3	% ±3
300	0.44	0.28	0.36		
77	0.54	0.30	0.38		
4.2	0.56	0.38	−0.15	48.0	52
	0.56	0.38	0.02	46.0	48

[a]IS, isomer shift; Γ, linewidth at half-height; SQ or 2ε, quadrupolar splitting; H_{hyp}, hyperfine field, %, proportion of each component.

The inverse magnetic susceptibility, which is plotted as a function of temperature in Fig. 7, gives clear evidence of paramagnetic behavior above 25 K and antiferromagnetic behavior below. The Curie constant, determined in the

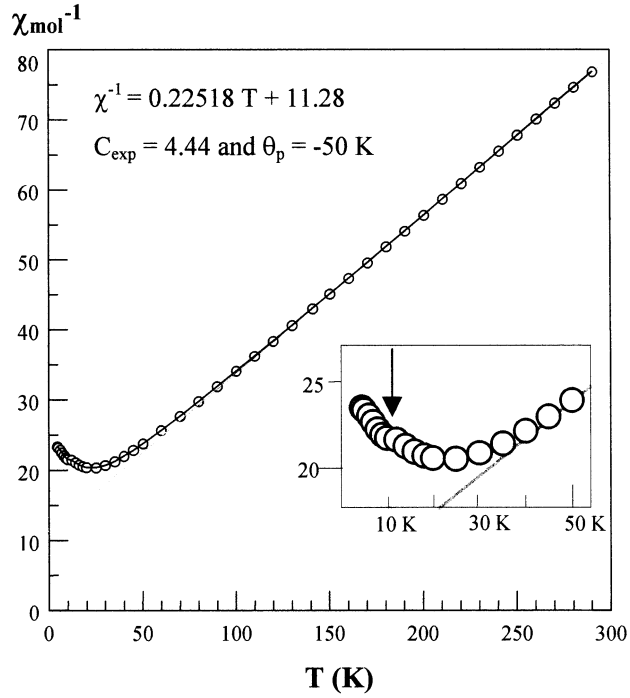

FIG. 7. Inverse magnetic susceptibility versus temperature (at H = 0.5 T) indicating antiferromagnetic behavior below 25 K. A small deviation is noticeable at ca. 11 K; it probably corresponds to a structural modification (see text).

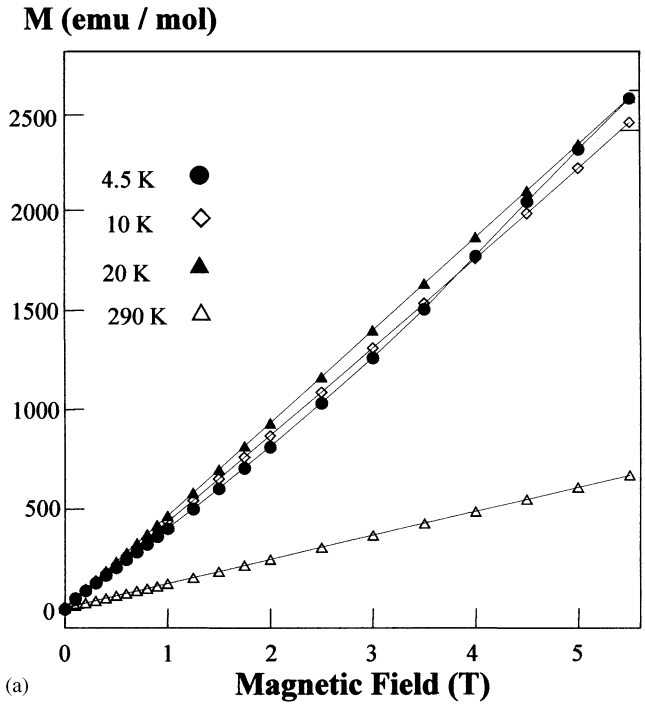

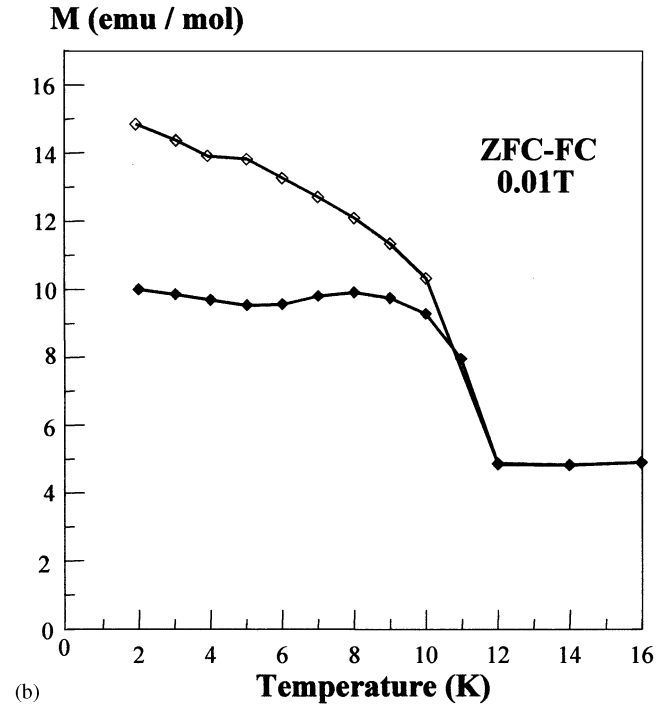

FIG. 8. (a) Magnetization versus applied magnetic field H at different temperatures. (b) Field-cooled and zero-field cooled magnetization curves.

range 100–300 K, is estimated at 4.4 and is well consistent with the theoretical spin-only value (4.37) for a high-spin-state Fe^{3+} cation; the paramagnetic Curie–Weiss temperature $\theta_p = -50$ K proves the presence of rather weak antiferromagnetic interactions. Below 25 K, a series of

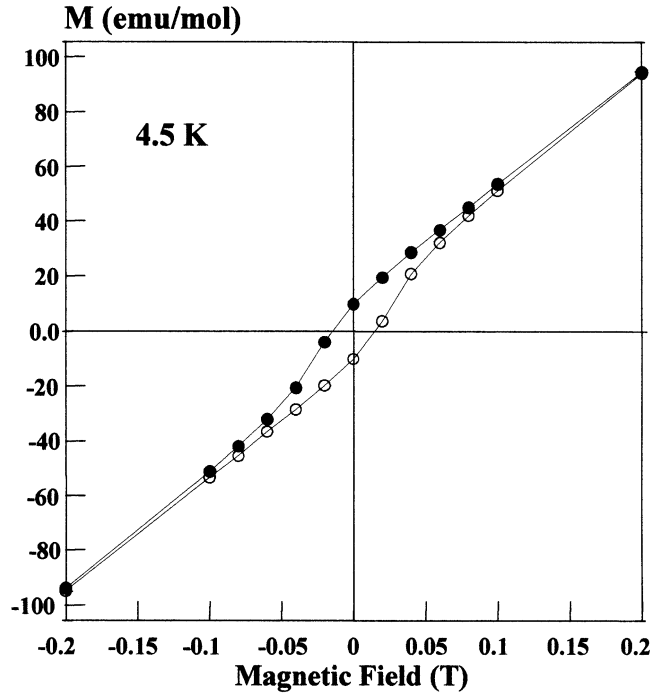

FIG. 9. Hysteresis loop at 4.2 K

magnetization curves were performed at different temperatures in addition to the temperature dependence of both field-cooled and zero-field-cooled magnetization, as illustrated in Figs. 8a and 8b, respectively. The latter clearly establishes that 3D magnetic ordering occurs at 11 K. The existence of a hysteresis loop ($H_c \sim 130/140$ Oe and $M_r \sim 0.05$ emu/g), represented in Fig. 9, indicates a canted antiferromagnetic behavior. However, the curious curvature of M(H) at 4.5 K cannot be explained. Finally, the shift in temperatures between the minimum of $1/\chi$ (25 K) and the collapse of FC and ZFC curves (11 K) suggests that 2D magnetic order is first established in the different layers between these two temperatures while the 3D magnetic order occurs below 11 K.

ACKNOWLEDGMENTS

The authors thank Dr. Marc Noguès (LMOV, Versailles) for magnetization measurements.

REFERENCES

1. S. T. Wilson, B. M. Lok, C. A. Messina, T. R. Cannan, and E. M. Flanigen, *J. Am. Chem. Soc.* **104,** 1146 (1982).
2. A. K. Cheetham, G. Férey, and T. Loiseau, *Angew. Chem. Int. Ed.* **38,** 3268 (1999) (b) M. Riou-Cavellec, D. Riou, G. Férey, *Inorg. Chim. Acta* **291,** 317 (1999).
3. S. S.-Y. Chui, S. M.-F. Lo, J .P. H. Charmant, A. Guy Orpen, and I. D. Williams, *Science* **283,** 1148 (1999).
4. S. O. H. Gutschke, M. Molinier, A. K. Powell, R. E. P. Winpenny, and P. T. Wood, *Chem. Commun.* 823 (1996).

5. (a) O. M. Yaghi, C. E. Davis, G. Li, and H. Li, *J. Am. Chem. Soc.* **119,** 2861 (1997). (b) H. Li, M. Eddaoudi, M. O'Keeffe, and O. M. Yaghi, *Nature* **402,** 276 (1999).
6. (a) F. Serpaggi and G. Férey, *J. Mater. Chem.* **8,** 2737 (1998). (b) F. Serpaggi, G. Férey, and E. Antic-Fidancev, *J. Solid State Chem.* **148,** 347 (1999). (c) C. Livage, C. Egger, M. Noguès, and G. Férey, *J. Mater. Chem.* **8,** 2743 (1998). (d) M. Riou-Cavellec, C. Albinet, C. Livage, N. Guillou, M. Noguès, J. M. Grenèche, and G. Férey, *Solid State Sci.,* in press. (e) K. Barthelet, J. Marrot, D. Riou, and G. Férey, *Angew. Chem. Int. Ed.* **49,** 281 (2002).
7. (a) F. Serpaggi and G. Férey, *J. Mater. Chem.* **8,** 2749 (1998). (b) M. Riou-Cavellec, C. Serre, J. Robino, M. Noguès, J.-M. Grenèche, and G. Férey, *J. Solid State Chem.* **147,** 122 (1999). (c) D. Riou, C. Serre, G. Férey, *J. Solid State Chem.* **141,** 89 (1998). (d) D. Riou, P. Baltazar, and G. Férey, *Solid State Sci.* **2,** 127 (2000). (e) Q. Gao, N. Guillou, M. Nogues, A. K. Cheetham, and G. Férey, *Chem. Mater.* **11,** 2937 (1999).
8. (a) D. A. Burwell and M. E. Thompson, *Chem. Mater.* **3,** 14 (1991). (b) B. Bujoli, A. Courillau, P. Palvadeau, and J. Rouxel, *Eur. J. Solid State Inorg. Chem.* **29,** 171 (1992). (c) P. Janvier, S. Drumel, Y. Piffard, and B. Bujoli, *C.R. Acad. Sci. Paris Ser. II* **320,** 29 (1995). (d) S. Drumel, P. Janvier, P. Bardoux, M. Bujoli-Doeuff, and B. Bujoli, *Inorg. Chem.* **34,** 148 (1995). (e) S. Drumel and M. Bujoli-Doeuff, *N. J. Chem.* **19,** 239 (1995). (f) F. Serpaggi, G. and Férey, *Inorg. Chem.* **38,** 4741 (1999). (g) M. Riou-Cavellec, M. Sanselme, J.-M. Grenèche, and G. Férey, *Solid State Sci.* **2,** 717 (2000).
9. (a) A. Distler and S. C. Sevov, *Chem. Commun.*, 959 (1998). (b) S. Ayyappan, G. Diaz de Delgado, A. K. Cheetham, G. Férey, and C. N. R. Rao, *J. Chem. Soc. Dalton Trans.*, 2905 (1999). (c) M. Riou-Cavellec, M. Sanselme, and G. Férey, *J. Mater. Chem.* **10,** 745 (2000). (d) N. Stock, G. D. Stucky, and A. K. Cheetham, *Chem. Commun.*, 2277 (2000). (e) M. Riou-Cavellec, M. Sanselme, N. Guillou, and G. Férey, *Inorg. Chem.* **40,** 723 (2001). (f) M. Riou-Cavellec, M. Sanselme, M. Noguès, J.-M. Grenèche, and G. Férey, *Solid State Sci.*, in press.
10. (a) G. B. Hix, D. S. Wragg, P. A. Wright, and R. E. Morris, *J. Chem. Soc. Dalton Trans.*, 3359 (1998). (b) J. Zhu, X. Bu, P. Feng, and G. D. Stucky, *J. Am. Chem. Soc* **122,** 11563 (2000). (c) N. Stock, S. A. Frey, G. D . Stucky, and A. K. Cheetham, *J. Chem. Soc. Dalton Trans.* 4292 (2000).
11. A. Goiffon, J.-C. Dumas, and E. Phillipot, *Rev. Chim. Miner.* **23,** 99 (1986).
12. G. M. Sheldrick, "SADABS: Program for Scaling and Correction of Area Detector Data." Univ. of Göttingen, 1996.
13. G. M. Sheldrick, "SHELXTL" version 5.10 "Software Package for Crystal Structure Determination," Siemens Analytical X-ray Instrument Inc., Madison, WI, 1994.
14. J. Teillet and F. Varret, "MOSFIT Program," unpublished.
15. N. E. Brese and M. O'Keeffe, *Acta Crystallogr. Sect. B* **47,** 192 (1991).
16. K. Nakamoto, "Infrared and Raman Spectra of Inorganic and Coordination Compounds," 5th ed. Wiley–Interscience, New York, 1997.